Fish and Shellfish Immunology 79 (2018) 140–152

Contents lists available at ScienceDirect

Fish and Shellfish Immunology

journal homepage: www.elsevier.com/locate/fsi

Full length article

Interferons type II and their receptors R1 and R2 in fish species: Evolution, structure, and function

Jiří Zahradník*, Lucie Kolářová, Hana Pařízková, Petr Kolenko, Bohdan Schneider**

Laboratory of Biomolecular Recognition, Institute of Biotechnology of the Czech Academy of Sciences, v. v. i., BIOCEV, Průmyslová 595, CZ-252 42 Vestec, Czech Republic

ARTICLE INFO

Keywords:
Interferon gamma
Type II interferons
Jak-Stat pathway
Fibronectin type III domain
Class 2 cytokine receptors
Fish immunity
Bioinformatics
Crystal structure
SAXS

ABSTRACT

Interferon gamma (IFN-γ) is one of the key players in the immune system of vertebrates. The evolution and properties of IFN-γ and its receptors in fish species are of special interest as they point to the origin of innate immunity in vertebrates. We studied the phylogeny, biophysical and structural properties of IFN-γ and its receptors. Our phylogeny analysis suggests the existence of two groups of IFN-γ related proteins, one specific for *Acanthomorpha*, the other for *Cypriniformes, Characiformes* and *Siluriformes*. The analysis further shows an ancient duplication of the gene for IFN-γ receptor 1 (IFN- γR1) and the parallel existence of the duplicated genes in all current teleost fish species. In contrast, only one gene can be found for receptor 2, IFN- γR2. The specificity of the interaction between IFN- γ and both types of IFN- γR1 was determined by microscale thermophoresis measurements of the equilibrium dissociation constants for the proteins from three fish species. The measured preference of IFN- γ for one of the two forms of receptor 1agrees with the bioinformatic analysis of the coevolution between IFN- γ and receptor 1. To elucidate structural relationships between IFN-γ of fish and other vertebrate species, we determined the crystal structure of IFN-γ from olive flounder (*Paralichthys olivaceus*, PoliIFN-γ) at crystallographic resolution of 2.3 Å and the low-resolution structures of *Takifugu rubripes, Oreochromis niloticus,* and *Larimichthys crocea* IFN-γ by small angle X-ray diffraction. The overall PoliIFN-γ fold is the same as the fold of the other known IFN- γ structures but there are some significant structural differences, namely the additional C-terminal helix G and a different angle between helices C and D in PoliIFN-γ.

1. Introduction

Interferons are proteins described by Isaacs and Lindenmann more than 60 years ago [1]. The name interferon is derived from the ability to interfere with viral infections. Interferons evolved in early chordates and represent ancient immunity elements [2]. Interferon gamma (IFN-γ) is now considered to be one of the key molecules in the regulation of the innate and adaptive immunity [3].

1.1. Interferon-γ and its signaling

IFN-γ is the only member of type II cytokines in mammals and plays a significant role in cell defense against intracellular pathogens. The IFN-γ function is best described in humans, where it mediates Th1 immunity and activates macrophages. The signaling of IFN-γ is initiated by the binding of the IFN-γ active form, a noncovalent homodimer, to receptor R1 [4–7] and subsequently to receptor R2 [8,9]. Formation of the IFN-γ/R1/R2 ternary complex results in spatial changes to cytoplasmic domains of receptors [10]. It leads to the binding of Janus activator kinase (JAK2) to the cytoplasmic part of receptor 2 and the attachment of JAK1 to the cytoplasmic part of receptor 1 [11], and the subsequent JAKs auto phosphorylation and phosphorylation of R1 [12,13]. This phosphorylation creates a binding site for the signal transducer and activator of the transcription (STAT1). After STAT1 is phosphorylated, it dimerizes and enters the cell nucleus where it induces expression of a variety of genes [14]. This sequence of events is described as the canonical pathway of IFN-γ signaling. So-called non-canonical IFN-γ signaling involves the endocytosis of the IFN-γ/R1/R2 complex, the creation of the IFN-γ/R1/STAT1α/JAK1/JAK2 complex and its transport to the nucleus. The IFN-γ nuclear localization signal (NLS) and polycationic C-terminus are crucial for the non-canonical IFN-γ signaling [15,16]. The IFN-γ/R1/Stat1α complex is responsible for the specificity of the interaction with the DNA regulatory sequences known as GAS - gamma interferon activation sites [17].

1.2. Interferon-γ in fish species

Teleost fish are an attractive target for studying evolution due to

* Corresponding author.
** Corresponding author.
E-mail addresses: jiri.zahradnik@ibt.cas.cz (J. Zahradník), bohdan.schneider@gmail.com, bohdan@ibt.cas.cz (B. Schneider).

https://doi.org/10.1016/j.fsi.2018.05.008
Received 15 February 2018; Received in revised form 27 April 2018; Accepted 2 May 2018
Available online 06 May 2018

their vast genomic variability [18]. During their evolution fish underwent three rounds of whole genome duplications (WGD) [19,20]. Two of these duplications are common to all vertebrates, the third one is specific for teleost fish. It occurred after fish and tetrapods split about 225–333 million years ago and it shows a specific evolutionary adaptation of fish [21]. Salmonid fish underwent one more WGD 96 million years ago [22], so did common carp (*Cyprinus carpio*) 12 Mya, [23]. In contrast to mammalian genomes, teleost genomes contain additional multiple families of active transposable elements which play an important role in the accelerated evolution of fish species [18]. Signaling pathway studies in fish provide important clues for understanding the evolution of specific immune adaptations of the antiviral defense system in early tetrapods and teleosts. Understanding the fish immune system may thus help the aquaculture industry's fight against fish viruses, whose occurrence remains a significant limiting factor in aquaculture production as well as in the sustainability of biodiversity in the world's oceans [24].

Type II interferon genes evolved early in the chordates evolution and are therefore present in extant cartilaginous fish (sharks and rays), bony fish, as well as in tetrapods [25]. It is assumed that they have evolved from a class II helical cytokine ancestor. Unlike humans with only one IFN-γ, the fish type II interferon family is broader in some species, consisting of two members, IFN-γ and fish-specific IFN-γ related (IFN-γrel) proteins. Moreover, in some fish species the *IFN*-γ gene is additionally duplicated resulting in two similar *IFN*-γ copies.

The first identified fish IFN-γ molecule was from the japanese pufferfish (*Takifugu rubripes*, Fugu) genome [26]. The *IFN*-γ gene was localized in the locus, which contains cytokine genes from the interleukin 10 family – *IL-22* and *IL-26*. These interleukins are tightly linked to *IFN*-γ in other species as well, including human, mouse, and frog. This fact supports the idea of gene synteny and helps *IFN*- γ identification in various genomes [21,27]. In salmonids and common carp, two *IFN*-γ genes are present likely due to the fourth WGD. Comparative studies of duplicated copies of *IFN*-γ were performed for atlantic salmon (*Salmo salar*) [28], common carp (*Cyprinus carpio*) [29] and rainbow trout (*Oncorhynchus mykiss*) [30]. Both IFN-γ paralogs appear to be biologically relevant and have a similar regulatory mechanism in these species.

Only some of the *IFN*-γ genes have been described at protein level. The FuguIFN-γ protein (UniProtKB - Q708J2) is expressed as 189 amino acid long pre-protein with the signal peptide 22 amino acids long and one potential glycosylation site. The gene composed of 3760 nucleotides (85% AT content) has 4 exons and 3 introns, which is similar to the composition of mammalian *IFN*-γ genes [26]. Approximately the same gene and protein characteristics were identified in rainbow trout (188 aa, AT rich) [31].

The biological functions of IFN-γ as well as its signaling pathways in fish are similar to those in mammals [31]. The highest expression level of IFN-γ has been found in the spleen, gill, and kidney of black seabream (*Acanthopagrus schlegelii*) [32] or zebrafish (*Danio rerio*) [33]. The IFN-γ expression is induced by various stimuli including lipopolysaccharides and poly I:C. IFN-γ has been shown to induce an inflammatory response and to protect the host from bacterial infection by stimulating the expression of genes of pro-inflammatory cytokines [31] in large yellow croaker (*Larimichthys crocea)* [34], atlantic cod (*Gadus morhua*) [35], nile tilapia (*Oreochromis niloticus*) [36], and atlantic halibut (*Hippoglossus hippoglossus* L.) [37].

1.3. Interferon-γ related protein in fish species

The comparative genomics analysis of the zebrafish and fugu genomes revealed the presence of a second *IFN*-γ gene in the locus containing interleukin 10 family genes. This gene was named interferon gamma 2 because of a low amino acid identity (17.0%) with the original *IFN*-γ gene [27]. The name interferon gamma related (*IFN-γrel*) gene was proposed later to distinguish between these two distinct genes and the highly similar *IFN*-γ copies in salmonids and cyprinids [38].

The IFN-γrel is not a clear homolog of the mammalian IFN-γ as identified by its gene synteny. Despite the sequence divergence, the genomic localization seems to be well conserved. Therefore, it is assumed that *IFN-γrel* originated by the duplication of the *IFN*-γ gene [21,27]. The IFN-γrel protein has been widely accepted as a second member of type II family [38]. Some hypotheses suggest that the novel IFN-γrel protein might have diverged, acquired a new function, and therefore have different affinities to the receptors [21,27]. The *IFN-γrel* gene has been identified mostly in the cyprinid family including zebrafish [27], grass carp (*Ctenopharyngodon idella*) [39], common carp [29], and gold fish (*Carassius aurutus* L.) [40], and also channel catfish (*Ictalurus punctatus*, *Siluriformes*) [41], and in fugu (*T. rubripes*, *Acanthomorpha*) [27]. C-termini of IFN-γrel sequences show significant differences, which indicates the existence of multiple IFN-γrel isoforms [31].

The zebrafish cDNA of the *IFN-γrel* gene encodes a 171-aa peptide with the 25-aa long signal sequence; the mature protein is 17.3 kDa in weight with two putative glycosylation sites [27]. Expression of common carp IFN-γrel protein was reported with N terminal 6xHis tag but without analysis of the protein [42].

The differences between IFN-γ and IFN-γrel signaling are poorly understood. The fish and human IFN-γ have analogical functions [43] and also IFN-γrel in *Cypriniformes* regulates antibacterial and antiviral activity. IFN-γrel is known not to be able to induce the genes of Toll-like receptors [44], and of interferon regulatory factors 1 [30] and 11 [38]. Studies of IFN- γrel bioactivity in ginbuna crucian carp (*Carassius auratus langsdorfii*) have reported that it is active as a monomer. This would be surprising because IFN-γ is known to function as a homodimer [45].

1.4. Interferon-γ receptors in fish species

Human IFN-γ induces a cell response through a receptor complex consisting of an IFN-γ homodimer and extracellular domains of two molecules of receptor 1 (IFN-γR1) and extracellular domains of two receptors 2 (IFN-γR2). The receptor molecules contain one conserved glycosylation site, an extensive cation-π motif in the D1 domain [9], and highly conserved cysteine residues capable of forming three potential disulfide bonds in R1 [46] and two in R2. All these signatures rank IFN-γ receptors into the class II receptor family with two fibronectin type III domains labeled D1 and D2 [47]. The intracellular part of receptors exhibits conserved potential phosphorylation sites. The phosphorylation sites are targeted by Jak1, Protein kinase C [48,49] and STAT1 [50] in the IFN-γR1, and by Jak2 [51] and leucine-leucine internalization motif in the IFN-γR2 [52].

Isoforms of interferon-γ receptors 1 and 2 were described in goldfish (*Carassius auratus* L.), zebrafish [40,53], rainbow trout, and stickleback (*Gasterosteus aculeatus*) [54]. Phylogenetic analysis places the teleost IFN-γR1 receptors separately from those of higher vertebrates and further still from IFN-γR2 sequences. IFN-γR1 exhibits higher expression levels than IFN-γR2 and a significantly higher expression in macrophages than in other cell types. The expression of IFN-γR2 is more tightly regulated than the expression of IFN-γR1. *IFN-γR2* gene synteny shows a conserved locus containing four clustered genes coding for *IFN-γR2*, interleukin 10 receptor beta (*IL-10RB*), interferon-α receptor 1 (*IFN-αR1*) and interferon-α receptor 2 (*IFN-αR2*) genes, similarly to the locus synteny in the human genome [54]. Two isoforms of IFN-γR1, named IFN-γR1-1 and IFN-γR1-2, were described in zebrafish and goldfish. An expression analysis in zebrafish tissues showed a significantly higher expression of IFN-γR1-1 than IFN-γR1-2, in goldfish there was a high expression of IFN-γR1-1 in the kidney and spleen, but also a high expression of IFN-γR1-2 in the brain [55]. Microscopy binding studies indicate that IFN-γR1-1 binds to IFN-γ1 but not to IFN-γR2, and IFN-γR1-2 preferentially binds to IFN-γrel [55].

1.5. Subject of this study

Even though the fish type II interferon system is actively studied, its many important aspects are still unknown. This is especially true for the biophysical studies of complex interactions between different type II interferons and their receptors. Here we report a thorough phylogeny study of IFN-γ, its receptors, and their co-evolution in fish species based on the combination of sequence and structure-based bioinformatics. The bioinformatic results are discussed in the light of the determined crystal structure of IFN-γ from olive flounder (PDB code 6F1E), the low-resolution topologies obtained by Small Angle X-ray diffraction (SAXS), and the binding affinities between IFN-γ and receptors of three species.

2. Methods

2.1. Expression and purification of recombinant IFN-γ proteins

Genes encoding for the interferon gamma proteins are detailed in Supplementary Material Table S1a; they are *Takifugu rubripes* TrubIFN-γ, Uniprot Q708J2, AA: 23–189; *Oreochromis niloticus* OnilIFN-γ, I3KNL7, AA: 23–206; *Paralichthys olivaceus* PoliIFN-γ, B3IXK1, AA: 24–198; *Ctenopharyngodon idella* CidIFN-γ2, gb AGG22551.1, AA: 26–182; *Epinephelus coioides* EcoiIFN-γ, gb AFM31242.1, AA: 22–200; *Larimichthys crocea* LcroIFN-γ, gb AIZ77177.1, AA: 22–200; variant of PoliIFN-γΔR with the C terminal deletion AA: 24–187. The genes were modified by a restriction enzyme site removal and optimization, obtained as DNA Strings (Thermo Fisher Scientific, Table S1a), and cloned to pET26b using restriction free cloning [56] or Transfer-PCR [57] in the position of *Nde*I and *Xho*I. All primers are listed in Table S1b. All used clones were verified by sequencing and single colony isolates were isolated by QIAprep® Miniprep Kit and used to transform expression hosts *E. coli* Rosetta™(DE3). Expression plasmids with OnilIFN-γ, TrubIFN-γ and PoliIFN-γ were deposited in Addgene plasmid repository (https://www.addgene.org/) under IDs 107287, 107288 and 107289 respectively. The cultures were grown in LB medium (1.0% tryptone, 0.5% yeast extract, 1.0% sodium chloride; pH 7.0) supplemented by trace elements TE (1 mM $MgSO_4$, 0.3 mM $CaCl_2$, 170 μM EDTA,30 μM $FeCl_3$, 6 μM $ZnCl_2$, 1 μM $CuCl_2$, 0.3 μM $CoCl_2$, 1 μM H_3BO_3, 70 nM $MnCl_2$) in 5 L Erlenmeyer flasks with 1 L of LBTE medium in Max Q 4000 shaker, Barnstead, Lab-Line (250 rpm, 30 °C). Heterologous expression was induced by 1 mM IPTG at OD_{600} of 0.6, the expression temperature was lowered to 16 °C and growth continued for 16 h. Cells were harvested by centrifugation (5000 g, 10 min, 4 °C) and stored in −20 °C for further use. Two-step purifications of interferons were based on SP Sepharose and gel filtration chromatography providing usually 10 mg/L of single band purity protein. Cells were disintegrated by sonication (Sonicator 3000, Misonix, 15–20 W) in buffer, (phosphate buffer saline, PBS: 137 mM NaCl, 2.7 mM KCl, 10 mM Na_2HPO_4, 1.8 mM KH_2PO_4) treated with 5 U/ml Benzonase® Nuclease, centrifuged (40 000 g, 4 °C, 30 min), and loaded on a HiTrap SP HP 5 ml (Ge Healthcare) column. Elution was performed by gradient 0–2 M NaCl (200 mM Na_2HPO_4, 50 mM NaH_2PO_4, 2 mM EDTA, 4 mM benzamidine, pH 7.3). Fractions with IFN-γ (eluted by high salt over 1 M NaCl) were immediately pooled and loaded on a HiLoad 16/600 Superdex 75 gel chromatography column pre-equilibrated in citrate buffer (100 mM, pH 6.0). All operations were performed on a NGC Chromatography system (Bio-Rad). The purified proteins were concentrated by Vivaspin Protein Concentrator Spin Columns to 10 mg/ml and directly used for crystallization or biophysical measurements. Identities of all expressed proteins were verified by mass spectrometry.

2.2. PoliIFN-γ protein crystallization and data collection

Crystals of PoliIFN-γ (Fig. S1) were grown using the hanging-drop vapor-diffusion method in a Greiner pre-greased 24 well Combo Plate with reservoir solution (optimized screen condition Index HT A9, Hampton research) consisting of 0.1 M Bis-Tris pH 5.5, 3 M NaCl and drops consisting mixture of 1 μl protein solution (10 mg/ml protein in 100 mM citrate buffer, pH 6.0) and 1 μl precipitant solution (the same as reservoir solution). After the growth during 2–3 days at ambient temperature (about 293 K), crystals were mounted in Round LithoLoops (Molecular Dimensions), some of them soaked with selenourea according to the method described previously [58], cryo-protected in 25% glycerol, and flash-cooled in liquid nitrogen.

Table 1
Data processing statistics and structure refinement parameters. Values in parentheses refer to the highest resolution shell.

	Native dataset	Selenourea soak
PDB code	6F1E	not deposited
Data processing statistics		
Wavelength (Å)	0.91841	0.97934
Space group	$P2_12_12_1$	$P2_12_12_1$
Unit-cell parameters a, b, c (Å); α, β, γ (°)	78.1, 78.1, 441.8 90.0, 90.0, 90.0	57.7, 83.0, 95.1 90.0, 90.0, 90.0
Resolution range (Å)	47.30–2.30 (2.38–2.30)	49.31–2.29 (2.37–2.29)
No. of observations	260,836 (24,236)	674,517 (57,880)
No. of unique reflections	20,255 (2032)	21,043 (1892)
Data completeness (%)	99.6 (97.4)	99.1 (92.1)
Average redundancy	12.9 (11.9)	32.1 (30.6)
Average I/σ(I)	13.5 (0.9)	18.9 (2.3)
Solvent content (%)	64.2	
Matthews coefficient (Å3/Da)	3.4	
Rmerge	0.102 (2.711)	0.138 (1.806)
Rpim	0.042 (1.163)	0.034 (0.455)
CC1/2	0.999 (0.559)	0.999 (0.737)
Structure refinement parameters		
Rwork	0.227	
Rfree	0.297	
Rall	0.229	
Average B-factor (Å2)	78	
RMSD bond lengths from ideal (Å)	0.014	
RMSD bond angles from ideal (°)	1.599	
Number of non-hydrogen atoms	2286	
Number of water molecules	38	
Ramachandran statistics: residues in favored regions (%); number of outliers	100; 0	

The X-ray diffraction data were collected at 100 K on the beamline MX 14.1 of the BESSY II synchrotron-radiation source at the Helmholtz-Zentrum Berlin (HZB). A native data set was collected at a wavelength of 0.918 Å, anomalous dispersion data set from a crystal soaked with selenourea were collected at a wavelength of 0.979 Å. The diffraction data statistics are shown in Table 1.

The PDB database (www.rcsb.org, [59]) was searched for the other IFN-γ structures using the Sequence & Structure Alignment and comparison tools; they are all mammalian: human, 1HIG [60], 1FG9 [5], 3BES [61]), rabbit *Oryctolagus cuniculus* 2RIG [62], and bovine *Bos taurus* 1D9C [63], 1RFB [64].

2.3. PoliIFN-γ data processing, structure determination and refinement

The diffraction data were processed using the XDS program package [65] and scaled using the program Aimless [66] from the CCP4 program package [67]. The positions of selenium atoms were found using the SHELX program package [68] using the data up to the resolution of 2.7 Å. Experimental phases were used in the program ARP/wARP [69] to build the initial model that was later used for structure determination using the native data set. Model building and manual corrections were performed using COOT [70], automated refinement procedures were performed using the program REFMAC [71]. The structure quality was

analyzed using MOLPROBITY [72]. The final structure parameters are shown in Table 1. The coordinates and structure factors have been deposited in the PDB [59] with the accession code 6F1E.

2.4. Expression and purification of recombinant IFN-γ receptor proteins

The extracellular parts of IFN-γ receptors of *P. olivaceus*, *T. rubripes*, and *O. niloticus* were produced by the Drosophila S2 expression system. The complete gene sequences, which were characterized in most cases as a putative protein, were acquired from the GenBank database, manually inspected by global alignments, shortened into extracellular parts only (chapter 2.8), and optimized for the *Drosophila* codons by the Life Technologies web optimization service. DNA Strings (Table S1a) were cloned into a modified pMT-BiP-V5-His_A vector using Gibson assembly [73] in the position *Bgl*II and *Xho*I restriction sites (Tables S1a and S1b). This procedure leads to the *IFN-γR1* genes in frame with the BiP signal peptides and C-terminal 6x HisTags. *Drosophila* Schneider S2 cells were transfected by using Effectene Transfection Reagent (Quiagen) according to the manufacturer's instructions together with selection plasmid pCoBlast. Stable cell lines were established by growing the S2 cells in HyClone SFX Medium supplemented with 10% FBS and 25 μg/ml Blasticidin S. The established cell lines were transferred and maintained in FBS-free SFX medium for expression batches. The protein expression was induced by addition of 1.0 mM $CuSO_4$. The cell-free medium (1 L) was prepared by centrifugation at 8000 g, 4 °C, 20 min and subsequently precipitated by addition of $CaCl_2$ to the final concentration of 5 mM, $NiSO_4$ (1 mM), NaCl (250 mM), and Tris-HCl, pH 8 (50 mM). This solution was centrifuged (10 000 g, 4 °C, 20 min) and filtered (0.45 μm) prior to the IMAC purification by standard procedure. Eluted fractions (300 mM imidazole) were directly loaded on the HiLoad 16/600 Superdex 75 (GE Healthcare) equilibrated by 10 mM Hepes, pH 7.5; 100 mM NaCl buffer. The samples were analyzed by 12% SDS-PAGE and verified by mass spectrometry.

2.5. Protein glycosylation and disulfide bond analysis

The protein glycosylation and S-S bond formation were determined by protein trypsinization in solution or in 12% SDS-PAGE and subsequent analysis by MALDI-MS according to the previously published methods [9,74,75].

2.6. Biophysical measurements

Circular dichroism (CD) spectra were acquired on the Chirascan-plus spectrometer (Applied Photophysics) with wavelength steps of 1 nm (185–260 nm) at 20 °C, protein concentrations of 0.1 mg/ml; the buffer spectra were subtracted. Results were analyzed by the CDNN software [76]. Protein melting curves were recorded by detecting the change of the tryptophan fluorescence at 330 and 350 nm between 20 °C and 95 °C (step 1 °C/min) with protein concentrations 1–3 mg/ml using Prometheus NT.48 (NanoTemper Technologies). Affinity measurements were performed by MicroScale Thermophoresis (MST) using a Monolith NT.115 instrument by NanoTemper Technologies. The receptors for IFN-γ from different species were labeled by the Monolith His-Tag Labeling Kit RED-tris-NTA provided by NanoTemper Technologies according to manufacturer's instructions. The labeled proteins were measured in a citrate buffer pH 6.0 at concentration of 200 nM with ranging concentration of a ligand and MST power 20–80%. Data from triplicates were analyzed by the MO.Affinity Analysis software version 2.1.2030.

2.7. Small angle X-ray diffraction experiments

The SAXS data were collected at the EMBL P12 beamline (DESY, Hamburg). Data were collected at 293.15 K at wavelength 1.24 Å with samples at four different concentrations. Sample to detector (PILATUS 2M, Dectris Ltd.) distance was 3.0 m, covering a scattering vector ($q = 4\pi\sin(\theta)/\lambda$) range from 0.0027 to 0.48 $Å^{-1}$. Data were collected, pre-processed and subtracted using the automated acquisition and analysis SAXS pipeline [77].

The scattering-derived parameters were determined using *PRIMUSqt r3709* [78], the pair-distance distribution function was determined using *GNOM v4.6.* [79]. The similarities of SAXS profiles were evaluated by the SIBYLS Beamline workflow (http://sibyls.als.lbl.gov/saxs_similarity/).

2.8. Sequence based bioinformatics

The known sequences of IFN-γ and IFN-γ receptors were downloaded from the NCBI Protein, UniProt and Ensembl databases (https://www.ncbi.nlm.nih.gov/protein/, http://www.uniprot.org/, http://www.ensembl.org/). The resulting set of sequences was used for pBLAST and tBLASTn (https://blast.ncbi.nlm.nih.gov/Blast.cgi, [80]) search of homologous proteins in bony fish species (taxid 7898). Multiple rounds of BLAST were performed in an iterative fashion: we started with sequences annotated as IFN-γ (IFN-γ R1, IFN-γ R2), and in each subsequent round, newly identified sequences with E-value above threshold 0.01 were added to the dataset and used for the next round of search. The procedure stopped when no yet unobserved sequences were found. In case the BLAST hit was genomic DNA without annotation, the genes and their products were predicted using the Exonerate software (version 2.2.0) [81]. Genes for fish IFN-γR2 were also identified among fish genomic sequences available at the NCBI Sequence Viewer 3.22.0 (https://www.ncbi.nlm.nih.gov/projects/sviewer/) taking advantage of their clustering with better annotated genes of the transmembrane protein 50B (*TMEM50B*). The sequences of the prospective IFN-γ and receptor proteins were manually checked and those that were truncated, duplicate or probably incorrectly based on alignment analysis were removed; the resulting list of the genes accepted for the analysis is provided in Supplementary Table S2a, the discarded ones in Table S3. Sequences from *Lepisosteus oculatus* (*Holostei*) were added to the datasets as outgroups, because *Holostei* diverged from the teleostean fish before the occurrence of the last, teleost-specific WGD.

The extracellular domains of IFN-γR1 and IFN-γR2 were predicted by the alignment using Muscle version 3.8.31 [82] with the sequences of human receptors and further validated by transmembrane helix localization by the TMHMM Server v. 2.0 [83] and by the SignalP 4.1 Server [84] (CBS Prediction Servers).

For phylogenetic analysis, the sequences of IFN-γ and the extracellular domains of IFN-γ receptors were aligned by Muscle version 3.8.31. Four sequences of IFN-γ (AHZ62713.1, KKF32167.1, XP_008399113.1, XP_014906354.1) were aligned separately from the rest because of their low sequence homology and added to the alignment using the Muscle "-profile" option. Aligned sequences were trimmed automatically by the trimAl tool (version 1.2rev59) with "–strict" option [85]. Phylogenetic trees were constructed by Bayesian inference using MrBayes 3.2.6 [86] with the best fitting model of evolution chosen by ProtTest 3.4.2 [87], and by a maximum likelihood approach using the online version of PhyML 3.0, (http://www.atgc-montpellier.fr/phyml/, [88]) with the substitution model selected by SMS [89] according to BIC, BIONJ starting tree, the NNI type of tree improvement and branch supports computed by aLRT SH-like. The trees were visualized and edited using FigTree (http://tree.bio.ed.ac.uk/software/figtree/) and TreeGraph 2 [90]. The similarities between results obtained by the different tree inference methods were computed by Compare2Trees, version September 2011 [91].

Coevolution between IFN-γ and its receptors was tested using the Parafit function [92] from the R package ape [93] with 999 permutations and the Cailliez correction for negative eigenvalues. Associations between all pairs of protein molecules coming from the same organism were tested. Results were visualized using the R package phytools [94]. Coevolution at amino acid level for IFN-γ and IFN-γR1 was investigated

using the i-COMS web-server [95] with MI, plmDCA, and mfDCA statistics. Multiple sequence alignments used as input were generated by Muscle from previously gained sequences according to i-COMS format requirements.

2.9. Structural bioinformatics

Structural comparisons and root-mean-square deviation (RMSD) values were calculated by MatchMaker as implemented in the UCSF Chimera software [96] with the Needleman-Wunsch algorithm and BLOSUM62 matrix. We used the BLOSUM 45-60, BLOSUM 80, and PAM matrices for very dissimilar or short sequences according to the Pearson rules [97,98]. The starting model for homology modeling was prepared by USF Chimera, the models were calculated by Modeller 9.19 [99,100] and the resulting structural alignment was used for the phylogeny study complemented by protein sequences of all known IFN-γ and receptor structures. The topology of the disulfide bonds was used as constrains for the modeling. To remove the effect of different mutual orientation of D1 and D2 domains of the extracellular parts of the receptors [9], the domains were modeled and aligned separately by using the known structures of the receptors [5,9,101]. For each sequence, two models were generated. Variable parts were re-modeled by the loop-refinement tool in Chimera and the DOPE-HR protocol [102].

3. Results and discussion

3.1. Summary of results

Fish IFN-γ were produced in *E. coli*, purified (Supplementary Fig. S1), characterized (Supplementary Figs. S2a and b), the crystal structure for PoliIFN-γ was solved at 2.3 Å resolution (PDB entry 6F1E, Fig. 1); the structures of other proteins were analyzed by the SAXS technique (Fig. S3). The phylogeny of IFN-γ and the receptors was subjected to comparison with fish evolution (Fig. 2) together with a further analysis of the components of the IFN-γ ternary complex: IFN-γ (chapter 3.3, Fig. 3 and Figs. S4a and b), IFN-γR1 (chapter 3.4, Fig. 3 and Figs. S5a and b) and IFN-γR2 (chapter 3.6, Fig. 3 and Figs. S6a and b). Fig. 4 displays the arrangement of gene clusters of IFN-γ and IFN-γR2. Finally, we describe the molecular coevolution between IFN-γ and its receptors (chapter 3.5) based on phylogeny (Fig. 5) and our biophysical experiments (Fig. S7).

3.2. Structure of PoliIFN-γ and the related IFN-γ

The interferons-γ PoliIFN-γ, OnilIFN-γ, TrubIFN-γ and LcroIFN-γ were produced from *E. coli* Rosetta (DE3) without the use of affinity tags in contrast to the previous studies of fish interferon gamma with TrxA (pET-32a), or N-terminal His tag [34] [42]. The purification protocol was set up on a SP Sepharose anion column in a similar manner as for human IFN-γ (Fig. S1) [7]. This procedure was very efficient due to the extreme pI of fish interferons (10.5 for PoliIFN-γ) and led to the overall yield of approximately 20 mg per L of *E. coli* culture. No or poor expression was obtained for CidIFN-γ2 and EcoiIFN-γ interferons. The PoliIFN-γ was also produced from S2 cells with some of the three potential glycosylation sites occupied by insect type of N-glycosylation, with a mass shift of approximately 3 kDa for monomer (SDS-PAGE analysis) but with very low yields (0.1 mg/L). Folding of all interferons was checked by CD spectroscopy and by measuring their melting temperatures (Fig. S2a).

Diffraction quality crystals were obtained only for PoliIFN-γ; the final construct was shortened by 11 amino-acids at the C terminus to obtain better diffracting crystals. The other interferons were prone to form non-diffracting needle-like structures. The structure of PoliIFN-γΔR (GenBank: BAG50577.1 [103]) was solved at 2.3 Å resolution by experimental phasing on PoliIFN-γ (wild type, 2.7 Å) using the selenourea labeling [58].

The PoliIFN-γ crystal structure is a homodimer with 175 amino-acids in each chain corresponding to the molecular weight of 2 × 20.4 kDa. The electron density map can be interpreted for 144 and 126 residues in chain A and B, respectively, both chains are quite similar with the root mean square deviation (RMSD) between 115 Cα pairs 0.75 Å. The amino acid residues 91–110, insertion characteristic for IFN-γ proteins from *Acanthomorpha*, are not resolved in the electron density.

The overall fold of PoliIFN-γ is similar to the fold of other known IFN-γ structures but significant differences were observed (Fig. 1). Most importantly, the first monomer of PoliIFN-γ is not composed of six α-helices as in all other known IFN-γ structures, but of seven. The additional α-helix unobserved in mammalian IFN-γ was resolved close to the C-terminus of chain A, the corresponding residues in chain B are disordered. The presence of this α-helix, labeled G in Fig. 1, is interesting in the light of the previously published speculation [21] about the interaction between the C-terminal amino acids and the receptor 1. The helix G can therefore play a role in the IFN-γ - receptor interactions.

Another feature distinguishing the PoliIFN-γ structure from the

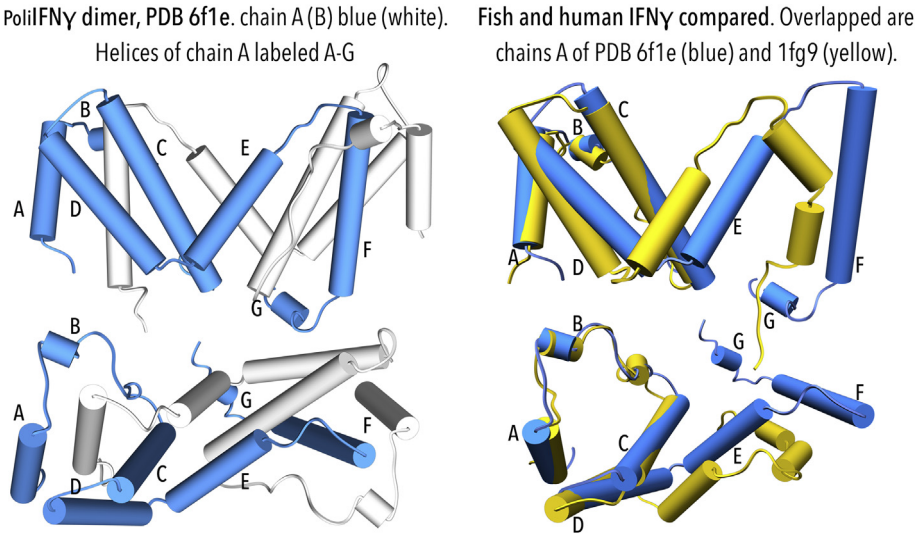

Fig. 1. Three-dimensional (3D) structure of the IFN-γ dimer from *Paralichthys olivaceus* (PoliIFN-γ, PDB 6f1e, this work, left), and the superposition of PoliIFN-γ and human IFN-γ (PDB 1FG9 [5], right). The α-helices are displayed as cylinders, top and bottom images are related by approximately 90° rotation.

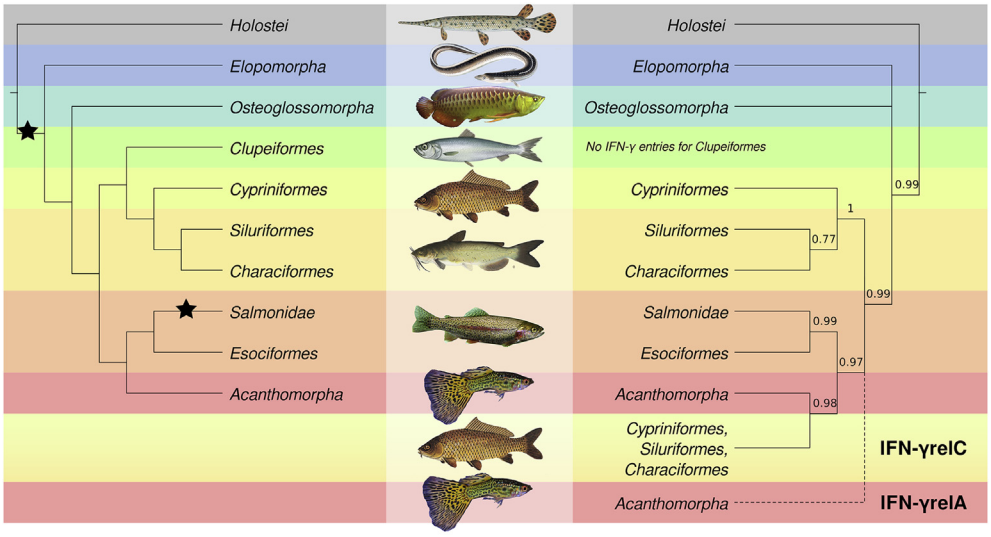

Fig. 2. Fish phylogeny (left, based on [104]) compared with the cladogram of fish IFN-γ and IFN-γ related proteins (right). Posterior probabilities of the internal branches computed by the MrBayes software are shown for the IFN-γ tree. Branches with posterior probability lower than 0.70 were collapsed. The position of the second cluster of *Acanthomorpha* sequences has low support and is thus unclear (marked by dashed line). The tree of fish phylogeny shows only orders with at least one representative of IFN-γ, IFN-γR1, or IFN-γR2 proteins in our set. There are no known IFN-γ, only IFN-γR1 entries for *Clupeiformes*. The stars mark the position of teleost-specific and salmonid-specific whole genome duplications [20] [19]. Pictures (from top to bottom): *Holostei: Lepisosteus oculatus*; *Elopomorpha: Anguilla japonica*; *Osteoglossomorpha: Scleropages formosus*; *Clupeiformes: Clupea harengus*; *Cypriniformes: Cyprinus carpio*; *Siluriformes: Ictalurus punctatus*; *Salmonidae: Oncorhynchus mykiss*; *Acanthomorpha: Poecilia reticulata*; *Cypriniformes: Cyprinus carpio*; *Acanthomorpha: Poecilia reticulata*; all fish pictures from Wikimedia Commons, edited.

known mammalian IFN-γ structures is the mutual orientation of helices D and E (Fig. 1). Repositioning of these helices in PoliIFN-γ, relative to the other IFN-γ structures, opens up their angle by almost 20° and results in the extension of the PoliIFN-γ structure. In consequence, neither of the PoliIFN-γ chains can be superimposed over the other known IFN-γ structures; RMSD between chains A of PoliIFN-γ and 1FG9 is 8.2 Å, and 7.5 Å for 1D9C when 121 (113) pairs of Cα atoms are considered. The close relationship between the IFN-γ molecules is observed when only the N-terminal helices A, B, C are superimposed; the RMSD values are 1.1 Å and 1.2 Å for the 40 Cα pairs for 1FG9 (Fig. 1) and 1D9C, respectively. The use of the Smith-Waterman algorithm and PAM matrices resulted in the identification of additional similarity regions among structures in loops between helix E and the first part of helix F (RMSD 0.58 Å for 19 pairs). Interestingly, the PoliIFN-γ structure is more similar to the human IFN-γ bound to receptor 1 (1FG9, [5]) than to the free form (1HIG [60]).

We measured the SAXS data of the expressed IFN-γ proteins to visualize their low-resolution structures. A comparison of the SAXS derived molecular envelope of PoliIFN-γ in solution with its crystal structure displays a general agreement. The similarity of the SAXS derived molecular envelopes of PoliIFN-γ and the other expressed fish IFN-γ proteins confirms that they all occur in solution as homodimers and it suggests their overall similarity (Fig. S3).

3.3. Evolution of IFN-γ and IFN-γrel proteins

We performed an extensive manual and computer alignment-driven search for all available IFN-γ sequences in fish species in the NCBI Protein, UniProt and Ensembl databases. The search yielded 63 sequences of IFN-γ and IFN-γ related proteins (Table S2) from 44 fish species, 28 of which were previously not correctly annotated as IFN-γ or IFN-γrel. One protein sequence was predicted by us from the genomic nucleotide sequence (Table S2b). The changes of annotations for all IFN-γ, IFN-γR1 and IFN-γR2 were recorded in Zebrafish Information Network (ZFIN, zfin.org) and were also submitted to the NCBI database. Based on our data, 18 new RefSeq database entries of IFN-γ and IFN-γrel, 55 new RefSeqs of IFN-γR1 and 30 new RefSeqs of IFN-γR2 were created. They are marked by bold font in Supplementary Table S2a. The new nomenclature introduced by ZFIN is *ifng1* for IFN-γ gene and *ifng1r* for IFN-γrel gene.

To uncover the evolutionary relationships between the retrieved IFN-γ sequences we conducted a phylogenetic analysis by the Bayesian

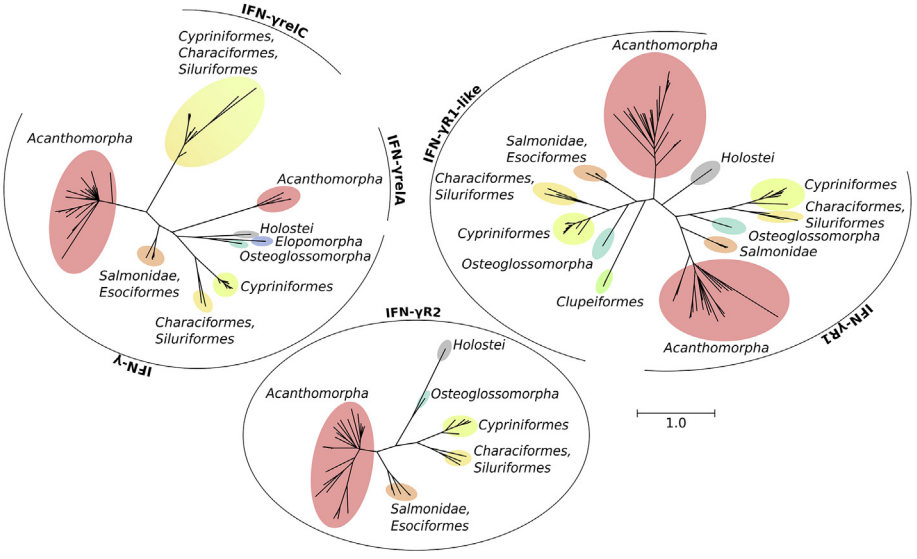

Fig. 3. Phylogeny of fish IFN-γ (top left), IFN-γ receptor 1 (top right) and IFN-γ receptor 2 (bottom). Branches with posterior probability lower than 0.5 were collapsed. The trees were computed by the Bayesian inference. Color scheme is analogous to Fig. 2. Details at the species level are given in Supplementary Figs. S4a and b; S5a, b and S6a, b. (For interpretation of the references to color in this figure legend, the reader is referred to the Web version of this article.)

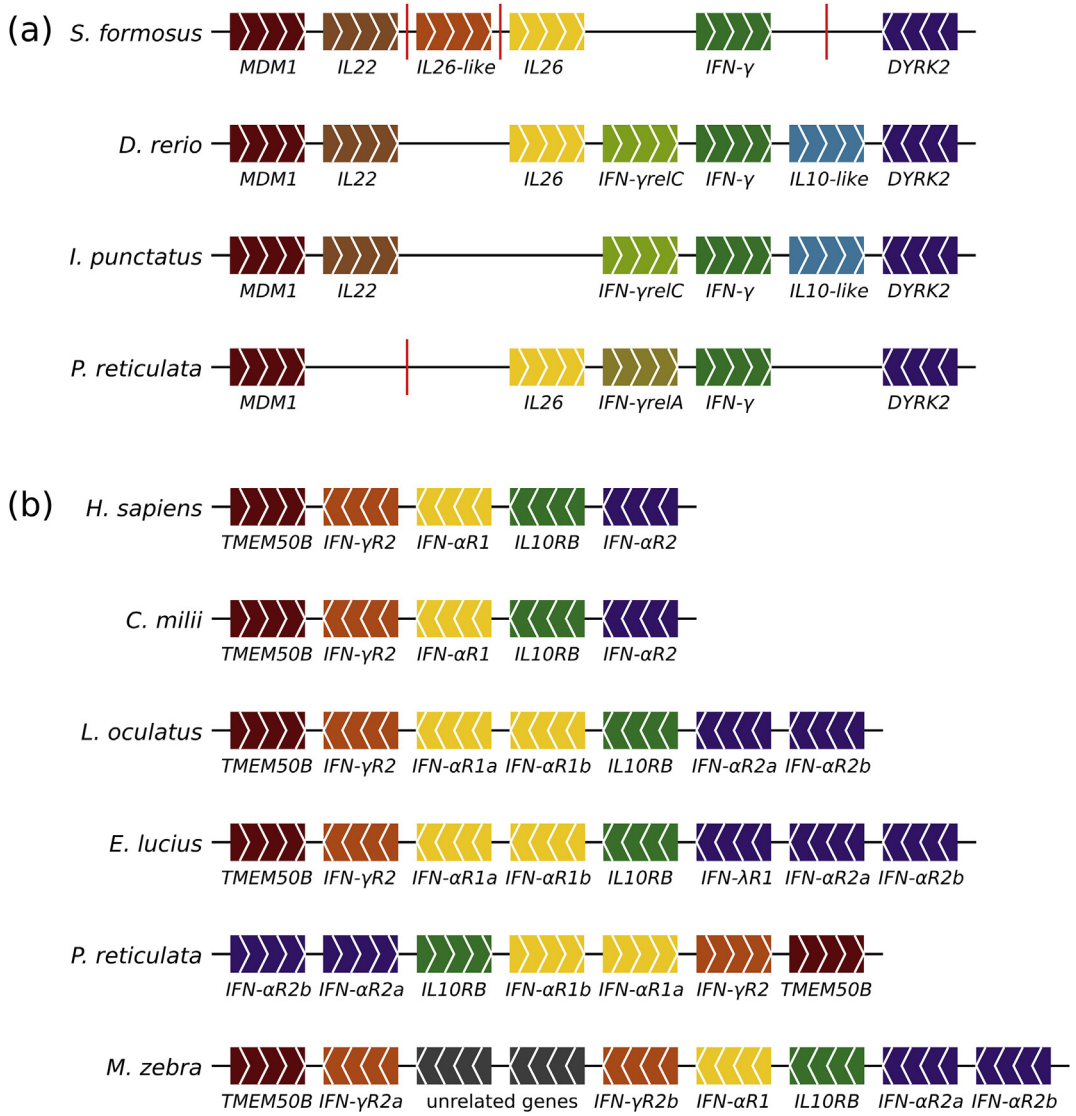

Fig. 4. *IFN-γ* and *IFN-γ receptor 2* gene clusters in different species, annotation according to the NCBI Sequence Viewer and mutual sequence homology. (a) *IFN-γ* genes in: *S. formosus*, *Osteoglossomorpha*; *D. rerio*, *Cypriniformes*; *I. punctatus*, *Siluriformes*; *P. reticulata*, *Acanthomorpha*. The cluster of *S. formosus* was constructed from two different scaffolds. (b) *IFN-γR2* genes physically co-localized in *H. sapiens* and selected fish species: *Homo sapiens*; *Callorhinchus milii*, *Chondrichthyes*; *L. oculatus*, *Holostei*; *Esox lucius*, *Esociformes*; *P. reticulata*, *Acanthomorpha, Cyprinodontiformes*; *Maylandia zebra*, *Acanthomorpha, Cichlidae*. The *E. lucius IFN-λR1* gene likely belongs to the *IFN-αR2* family despite that it is annotated as interferon-λ receptor 1. The two grey colored genes in *M. zebra* genome are likely not analogous to any other gene in the cluster and the function of their products is unknown [107]. The white arrows mark the orientation of genes, the red vertical lines indicate that the genome sequence is incomplete in this position. The lengths of genes and intergenic regions are not to scale. Only protein-coding genes are shown. The exact genomic locations and the gene identifications are listed in Tables S4a and c. (For interpretation of the references to color in this figure legend, the reader is referred to the Web version of this article.)

inference (Figs. 2 and 3 and Fig. S4a) and maximum likelihood methods (Fig. S4b) according to the previously published computations [105,106]. The topologies of the trees calculated by these two methods reflect fish phylogeny quite well and are quite similar. Differences were located only at the level of species and genera; the similarities were 84% for IFN-γ, 94% for IFN-γR1 (chapter 3.4), and 86% for IFN-γR2 (chapter 3.6). The phylogeny is summarized in Fig. 2, more details can be found in Figs. S4a, b, S5a, b (IFN-γR1), and S6a, b (IFN-γR2).

Fig. 3 summarizes our phylogenetic calculations of IFN-γ and its two receptors. The analysis shows clear separation of IFN-γ and IFN-γrel into two clearly separated paralogs of human IFN-γ ("canonical IFN-γ"). IFN-γrel then forms two distinct clusters - one comprises proteins of *Cypriniformes*, *Siluriformes,* and *Characiformes* orders (further referred to as IFN-γrelC), the other was detected in *Acanthomorpha* (IFN-γrelA).

To test the possibility that IFN-γrel proteins form two independent groups, we looked at the *IFN-γ* gene locus structure (Fig. 4a). In genomes of *D. rerio* (*Cypriniformes*), *I. punctatus* (*Siluriformes*), *Astyanax mexicanus* (*Characiformes*) and *P. reticulata* (*Acanthomorpha*) the *IFN-γ* and *IFN-γrel* genes are adjacent and in the same orientation (Fig. 4a – II-IV, data for *A. mexicanus* not shown), while there is no annotated gene in this location in the genome of *S. formosus* (*Osteoglossomorpha*) (Fig. 4a – I). This could be the result of three different scenarios: 1. The *IFN-γ* gene was duplicated once prior to the teleostean split and the second copy has been lost in *S. formosus*. 2. The *IFN-γ* gene was duplicated once after *Osteoglossomorpha* have diverged from the rest of teleosts. 3. The IFN-γrel of *Cypriniformes* and IFN-γrel of *Acanthomorpha* originated in two independent duplications of the *IFN-γ* gene. Further investigation is needed to decide, which of these hypotheses is true. The hypothesis of single IFN-γ gene duplication that occurred prior to the teleostean diversification [27] cannot be dismissed, because we could identify only 4 IFN-γrelA sequences that had a low sequence homology compared to the rest of the set and the position of their subtree (Fig. 3)

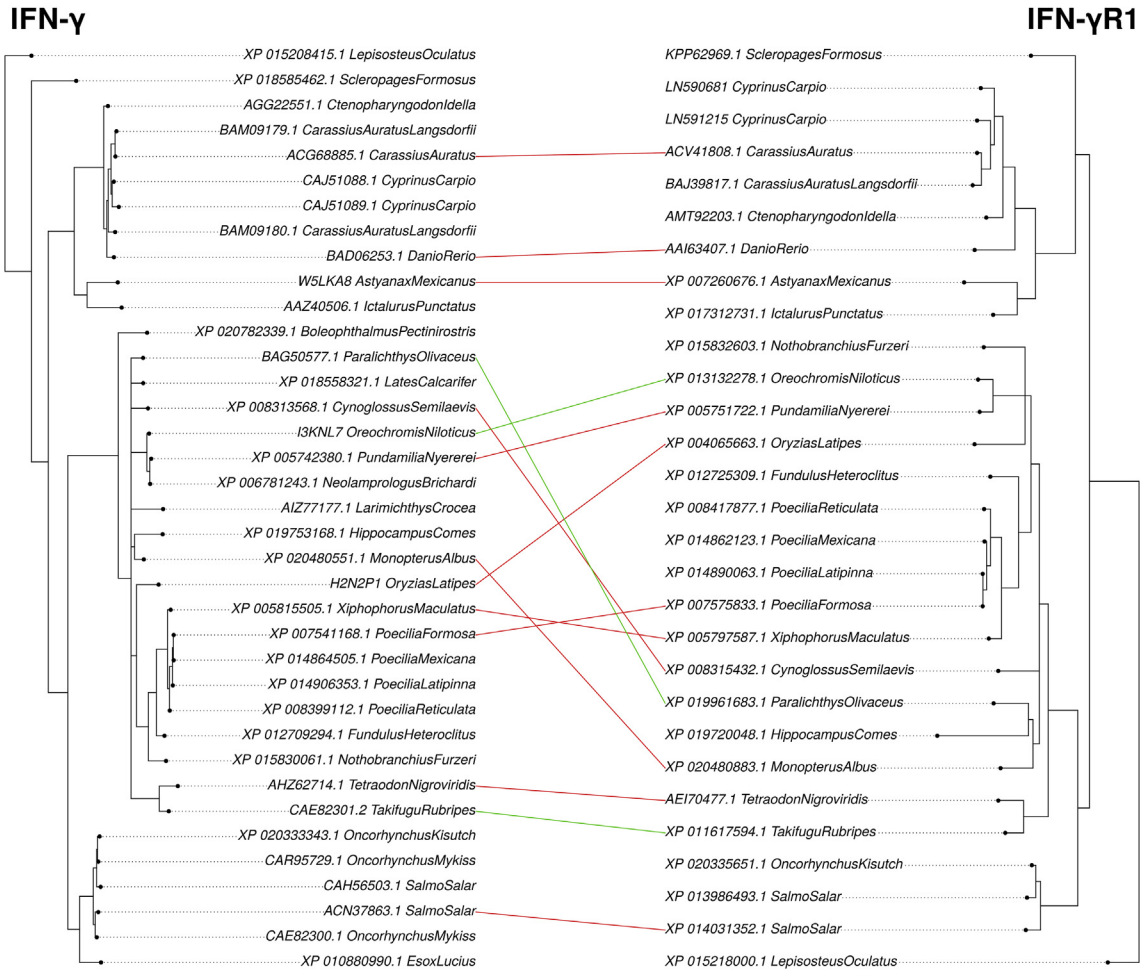

Fig. 5. The analysis of phylogenetic coevolution of IFN-γ (left) and IFN-γR1 (right). Trees computed by the Bayesian inference were used, branches corresponding to IFN-γrelA and IFN-γrelC were removed from the IFN-γ tree. All links between the receptor and ligand from the same species were tested. Significant evolutionary links are shown as red lines. A link was considered significant if the p-value of both test statistics implemented in the Parafit function was lower than 0.1. Experimentally tested pairs of IFN-γ and IFN-γR1 are shown as green lines; all three are not significant. (For interpretation of the references to color in this figure legend, the reader is referred to the Web version of this article.)

had a low statistical weight. Also, the question remains whether all *Acanthomorpha* have the IFN-γrelA protein, or if it occurs only in some species from this largest group of present fish species.

Salmonidae fish also possess two different IFN-γ proteins. However, these proteins are highly similar (over 90% of amino acid identity for *O. mykiss* and *S. salar*) and thus form only one cluster in the phylogenetic tree (Figs. S4a and S4b). These proteins likely originated in the last whole genome duplication, which *Salmonidae* underwent approximately 96 Mya [22]. Similarly, two different sequences of IFN-γ and two sequences of IFN-γrel in tetraploid *C. carpio* [23] result from the recent whole genome duplication (approx. 12 Mya) and a more recent wave of segment duplications (2.3–6.8 Mya).

3.4. Phylogeny of fish IFN-γ receptor 1

The database and BLAST search yielded 96 sequences of IFN-γ receptor 1 (Table S2a), 60 of them were previously not annotated as such. The sequences come from 44 different fish species, 32 of which were also represented by at least one representative in the IFN-γ dataset. Most of the species are represented by two distinct IFN-γR1 protein sequences, the observation has already been published for *C. auratus* and *D. rerio* [55]. The available data indicate that the IFN-γR1 protein is represented by two distinct genes in all fish orders except the evolutionary oldest one, *Holostei*. These two IFN-γR1 proteins are not close isoforms; their overall amino acid identity is below 30% (Table 2). Moreover, additional close IFN-γR1 isoforms have been identified in the genome of *C. carpio* [108], *O. kisutch*, *Sinocyclocheilus grahami*, *S. anshuiensis*, *S. rhinocerous*, and *Clupea harengus*, in the first five cases probably as a result of duplication of the whole genome.

We performed a phylogenetic study for all found sequences of the extracellular domain of IFN-γR1. Intracellular domains have been excluded from the comparison because of their low sequence homology. The IFN-γR1 sequences are split into two independent clusters (Fig. 3, Figs. S5a and S5b), as expected from their low sequence homology. Further on, these two groups are named IFN-γR1 and IFN-γR1-like as in the ZFIN database. The genes of IFN-γR1 and IFN-γR1-like groups are located on different chromosomes in genomes of fish species spanning across the whole teleostean phylogenetic tree (Table S4b). Thus, it is likely that the origin of the second IFN-γR1 copy lies in the teleost-specific whole genome duplication.

3.5. Coevolution between IFN-γ and IFN-γ receptors

Having two homologs of IFN-γ (canonical IFN-γ and IFN-γrel) and two homologs of IFN-γR1, a question arises what ligand-receptor pairs signal. The previous *in vitro* [55] and *in vivo* [53] results have suggested that canonical IFN-γ binds preferably to IFN-γR1-like (designated also as Crfb13), but not to IFN-γR1 (Crfb17), while both IFN-γR1 and IFN-γR1-like are important for IFN-γrelC signaling. We decided to test this hypothesis both programmatically by searching for the coevolution of

Table 2
Amino acid identity of the two distinct IFN-γR1 receptors of selected fish species.

Species	Order	IFN-γR1 NCBI protein ID	IFN-γR1-like NCBI protein ID	Amino acid identity %
Scleropages formosus	*Osteoglossomorpha*	KPP62969.1	XP_018604991.1	28
Danio rerio	*Cypriniformes*	AAI63407.1	NP_001165063.1	23
Ictalurus punctatus	*Siluriformes*	XP_017312731.1	XP_017319969.1	21
Oncorhynchus kisutch[a]	*Salmonidae*	XP_020335651.1	XP_020315962.1, XP_020315966.1	28/28
Poecilia reticulata	*Acanthomorpha*	XP_008417877.1	XP_008427408.1	27
Tetraodon nigroviridis	*Acanthomorpha*	AEI70477.1	AEI70478.1	25

[a] The dataset contains three IFN-γR1 sequences for *Oncorhynchus kisutch*. Two of them are highly similar, the amino acid identity indicates the similarity of the two close homologous sequences with the third one.

Table 3
The interaction affinities of the IFN-γ proteins and the extracellular parts of their receptors 1. The affinities were measured as equilibrium dissociation constants Kd by microscale thermophoresis. All interactions between IFN-γ and receptors 1 from different species have Kd values larger than 20 μM. The previous SPR experiment with the human proteins determined the Kd value as 31 ± 1 nM [7].

Interaction partners	Kd for IFN-γR1 [nM]	Kd for IFN-γR1-like [nM]
PoliIFN-γ	123 ± 15	321 ± 23
TrubIFN-γ	106 ± 8	384 ± 42
OnilIFN-γ	136 ± 8	317 ± 34
humanIFN-γ	41 ± 1	–

the receptor-ligand pairs, and experimentally by biophysical measurements of the equilibrium dissociation constants (Kd; Table 3 and Fig. S7).

We computationally tested the coevolution between: (i) IFN-γ and IFN-γR1; (ii) IFN-γ and IFN-γR1-like; (iii) IFN-γrelC and IFN-γR1, and (iv) IFN-γrelC and IFN-γR1-like. We also performed tests of coevolution between *Cypriniformes* IFN-γ and both IFN-γR1 and IFN-γR1-like to compare it with the results for IFN-γrelC. Similar tests for IFN-γrelA were not performed due to a low number of sequences (4) available for this group. IFN-γ showed no significant coevolution with either IFN-γR1 or IFN-γR1-like, however, the test statistics are much higher (and thus the proteins are more likely to have coevolved) for the relationship with IFN-γR1 (p-value = 0.078 for IFN-γR1; p-value = 0.421 for IFN-γR1-like). In addition, no coevolving pairs were discovered for IFN-γ and IFN-γR1-like proteins, while there were 11 significantly coevolving pairs observed for IFN-γ and IFN-γR1 proteins (Fig. 5). IFN-γrelC shows significant coevolution with IFN-γR1-like (p-value = 0.028), but not with IFN-γR1 (p-value = 0.198), while *Cypriniformes* IFN-γ showed no significant coevolution with either IFN-γR1 or IFN-γR1-like. Our results are thus not in an agreement with the previous results [53,55], as they support the hypothesis that IFN-γ binds to IFN-γR1, while the evolution of IFN-γrelC is driven mainly by its relation with IFN-γR1-like.

The binding affinities between IFN-γ and receptor 1 were measured by microscale thermophoresis (MST). In agreement with our coevolution computations, the MST determined that Kd values show stronger binding between IFN-γ and receptors R1 with an average affinity around 100 nM (Table 3). The Kd of receptors R1-like proteins have significantly weaker binding affinities and Kd values above 300 nM (Table 3). However, the observed differences in Kd values are within one order of magnitude and can be overcome by avidity or concentration effects on the cell surfaces. Receptor concentration on the cell surface is not known and can differ significantly according to the cell type or cell's previous activation. Situation is even more complex if we take into account the function of the receptors. Receptors 1 (R1 and R1-like) serve as high affinity binders but the signalization is finally triggered by low affinity receptors 2. Therefore, the biological function may be determined not only by the affinities of receptor 1.

3.6. Phylogeny of fish IFN-γ receptor 2

At the time of this study, only three fish IFN-γR2 proteins were annotated in the public databases (*L. oculatus*, *Holostei*; *O. mykiss*, *Salmonidae*; *S. salar*, *Salmonidae*) and their sequential similarities were not sufficient to search for more IFN-γR2 genes by BLAST. We therefore decided to search for potential *IFN-γR2* genes using their genomic location. In the human genome, the *IFN-γR2* gene is clustered with genes coding for *IFN-λR2*, *IL10RB*, *IFN-λR1* and the transmembrane protein 50B (*TMEM50B*) (Fig. 4b). The locus structure remains the same for cartilaginous fish *C. milii* (*Chondrichthyes*) and is very similar also in *L. oculatus* (*Holostei*). Thus, we have benefited from the gene synteny and searched for the *IFN-γR2* gene in fish genomes using a better annotated gene *TMEM50B*. This procedure and the subsequent rounds of BLAST searches yielded 43 different IFN-γR2 sequences coming from 38 fish species.

The structure of the *IFN-γR2* locus is quite diverse among different fish species (Fig. 4b). The phylogenetic trees of the extracellular domains of fish IFN-γR2 computed by the Bayesian inference and maximum likelihood approach (Fig. 3, Figs. S6a and b) are almost identical (86% similarity, chapter 3.3) and both trees match almost exactly the evolution of fish. There are only two differences: (i) the presence of two distinct groups of *Salmonidae* IFN-γR2, whose origin most probably lies in the Salmonid-specific whole-genome duplication, and (ii) the presence of two distinct IFN-γR2 molecules for *Cichlidae* species (Table S3). The *Cichlidae* IFN-γR2 proteins for *O. niloticus*, *Haplochromis burtoni*, and *M. zebra* are colocalized, possess over 90% amino acid identity, and form one cluster in the phylogenetic tree. Therefore, the two genes for IFN-γR2 are likely the consequence of a recent gene duplication event.

The global test of coevolution of IFN-γR2 with IFN-γ was not statistically significant (p-value 0.13), but this result is not surprising due to the low expected binding affinity between IFN-γR2 and IFN-γ [109]. On the other hand, IFN-γR2 seems to be coevolving with both IFN-γR1 and IFN-γR1-like (p-values 0.02 and 0.05). Our previously discussed data suggest that IFN-γ signals by interacting with IFN-γR1 and IFN-γrel signals by interacting with IFN-γR1-like. The significant coevolution of IFN-γR2 with both IFN-γR1 and IFN-γR1-like then implies that IFN-γR2 is involved in signaling of both IFN-γ and IFN-γrel. The promiscuity of the second receptor is a common feature for receptors of the closely related interleukin 10 family [109,110]. However, we cannot rule out the existence of the second IFN-γR2 molecule if its gene was located in a different locus; in any case, this putative gene sequence would be dissimilar from sequences of the known IFN-γR2. An indirect support for the existence of a second IFN-γR2 are the previously published experimental results [53], according to which IFN-γR2 (termed there Crfb6) is important for IFN-γrelC signaling, but not for IFN-γ signaling.

Our attempts to compute the receptor-ligand co-evolution at amino acids level by i-COMS web-server [95] and correlate its results with structural models failed. The majority of coevolving pairs were core-associated rather than intermolecular, which has been reported previously [111]. The coevolution between fish IFN-γ and its receptors is driven by frequent remodeling of the structure in the loop regions,

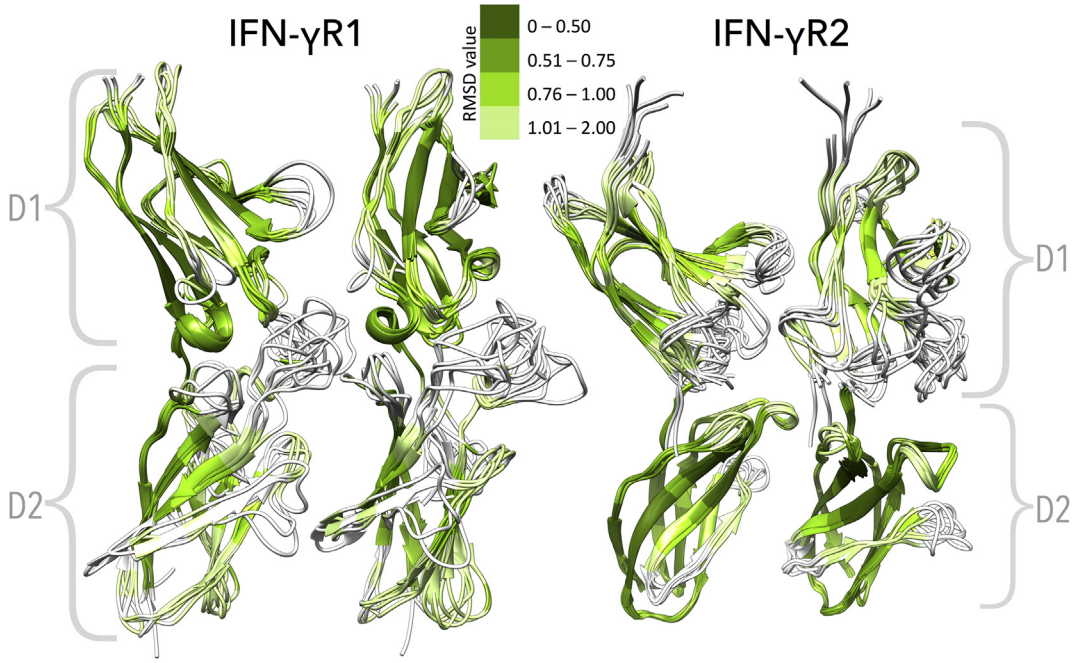

Fig. 6. Computer models of structures of the PoliIFN-γR1, TrubIFN-γR1, OnilIFN-γR1 (a) and PoliIFN-γR2, TrubIFN-γR2, OnilIFN-γR2 (b). The PoliIFN-γR1 model was based on structure of the human receptor 1 (1FG9 [5]), PoliIFN-γR2 model on structure of the human receptor 2 (5eh1 [9]). The RMSD color scheme shows the closeness of the modeled receptors to their respective template crystal structures. The models were built by minimization using the default setting in Chimera [96]. (For interpretation of the references to color in this figure legend, the reader is referred to the Web version of this article.)

which is caused by insertions or deletions in the gene (Fig. S8).

3.7. Computer modeling of the structures of IFN-γ receptors 1 and 2 and their binding interfaces with IFN-γ

The molecules of IFN-γ receptors 1 and 2 are composed of two immunoglobulin-like β-sheet domains called D1 and D2, both with fibronectin type-III topology (Pfam PF00041) [5,9]. The topologies of both domains are well conserved among class 2 cytokine receptors [112] [113]. The D1 domains are composed of three β-strands stacked on a layer of four β-strands that form sandwich-like structure and are also characteristic by an extensive cation π-stacking motif and one structurally conserved S-S bond [9]. The D2 domains form a similar β-sandwich structure with four β-strands stacked on the remaining four β-strands. This core of the class 2 cytokine receptors is fairly uniform and our sequence alignments support their existence also in fish receptors.

Homologous models of the structures of IFN-γ receptors 1 and 2 (Fig. 6) were built for the expressed proteins from species *P. olivaceus*, *T. rubripes*, and *O. niloticus*. The models of IFN-γR1 were computed based on the human (pdb 1FG9 [5]) and chicken (pdb 4EQ2, 4EQ3 [101]) structures of receptor 1 by using UCSF Chimera [96] and Modeller 9.19 [99,100]. The S-S bond formation patterns were used as constraints for the modeling (Fig. S2b). The models showed two expected Fibronectin type III domains with a majority of significant structural changes located in the loop L6 of the D2 domain (in 1FG9 residues 138–148). At the same time, the RMSD of the core parts of the compared proteins were below 1 Å. The structurally most variable part in our models of IFN-γR1 corresponds to the loop L6, which forms the recognition interface with the IFN-γ loop AB and helices B and F'. This is consistent with the assumption that the IFN-γ/IFN-γR1 recognition is controlled by the three loops located between the receptor 1 domains D1 and D2 [114] and by their mutual orientation [9]. We therefore assumed that the corresponding parts of the fish proteins contribute in a similar mutual position to the IFN-γ/R1 recognition.

Models of the second receptor IFN-γR2 were generated by the same methodology, using the crystal structures of human IFN-γR2 (pdb 5eh1 [9]) considering also IL10RB (pdb 3lqm [109]). In contrast to the IFN-γR1 models, most structural changes in the models of IFN-γR2 were identified in two D1 domain loops (residues 48–56, 70–81 in 5EH1).

4. Conclusions

Our bioinformatic analysis of IFN-γ and the extracellular parts of its two receptors disclosed unexpected diversity of sequences and revealed new attributes of evolution of this essential immunity signaling pathway in fish species. Our sequence database mining resulted in newly identified or annotated genes coding for the proteins participating in the IFN-γ signaling system: 28 IFN-γ and IFN-γrel, 60 IFN-γR1, and 40 IFN-γR2. The phylogeny of IFN-γ protein genes confirmed the existence of a group of proteins closely related to but distinct from IFN-γ named IFN-γrel. We discovered that there are likely two independent groups of IFN-γrel proteins: IFN-γ relC occurring in *Cypriniformes, Characiformes* and *Siluriformes* and IFN-γrelA occurring in *Acanthomorpha*.

Similarly to the existence of two groups of IFN-γ, the phylogeny and sequence alignments of IFN-γ receptors 1 manifest the existence of two independently evolving groups of genes labeled IFN-γR1 and IFN-γR1-like. The specificity of the binding between IFN-γ and the two types of IFN-γR1 was tested computationally by the tightness of their coevolution, and by the biophysical measurements of affinities between pairs of these proteins from three fish species (Table 3). Our coevolution studies as well as the measurement of affinities show that IFN-γ has a higher affinity for IFN-γR1 than for IFN-γR1-like so that the latter molecule is likely diverging from the original function. In contrast to IFN-γ and IFN-γR1, there is no sign of existence of two separate IFN-γR2 genes. However, this possibility cannot be ruled out in case the gene for the putative second R2 group is dissimilar and located in a different locus.

In summary, we have shown that three functionally tightly linked molecules, IFN-γ, IFN-γR1, and IFN-γR2, have probably underwent distinct evolutionary events: (i) IFN-γ being duplicated independently in at least two groups of fish; (ii) IFN-γR1 being duplicated once and preserved in both copies in all the descendants; (iii) IFN-γR2 probably

not being duplicated at all. The differences between the IFN-γ signaling in fish and mammals are illustrated by the graphical abstract.

An independent insight into IFN-γ evolution has been achieved by solving the crystal structure of IFN-γ from *Paralichthis olivaceus*. The structure of the PDB accession code 6F1E was solved by selenourea experimental phasing and revealed a fold observed in IFN-γ molecules from mammalian species: a homodimer composed of two four helix bundles. The structure however shows significant differences. Most notably, one PoliIFN-γ monomer exhibited an additional helix G at the C terminus and the dimer is more extended compared to the mammalian counterparts because the angle between helices C and D opens it up (Fig. 1). The information based on the crystal structure of PoliIFN-γ was complemented by measuring the solution SAXS data of IFN-γ proteins from three fish species and confirmed the dimeric form and shapes compatible with the shape of the known IFN-γ crystal structures.

We believe that our phylogeny work and the solved crystal structure of PoliIFN-γ helps the understanding of the complex phenomenon of IFN-γ evolution in fish species and of early stages of immunity development in vertebrates.

Acknowledgments

This study was supported by the Czech Science Foundation grant 16-20507S and by the projects New research methods to BIOCEV (CZ.1.05/2.1.00/19.0390), and CIISB (LM2015043, and CZ.02.1.01/0.0/0.0/16_013/0001776) from the ERDF. It was conducted at the Institute of Biotechnology CAS with the help of the institutional grant RVO 86652036. We thank HZB and EMBL for the allocations of a synchrotron-radiation beamtime.

Appendix A. Supplementary data

Supplementary data related to this article can be found at http://dx.doi.org/10.1016/j.fsi.2018.05.008.

References

[1] A. Isaacs, J. Lindenmann, Virus interference. I. the interferon, Proc. Roy. Soc. Lond. B Biol. Sci. 147 (927) (1957) 258–267.
[2] S. Pestka, The interferons: 50 years after their discovery, there is much more to learn, J. Biol. Chem. 282 (28) (2007) 20047–20051.
[3] J.R. Schoenborn, C.B. Wilson, Regulation of interferon-gamma during innate and adaptive immune responses, Adv. Immunol. 96 (2007) 41–101.
[4] M. Fountoulakis, J.F. Juranville, A. Maris, L. Ozmen, G. Garotta, One interferon gamma receptor binds one interferon gamma dimer, J. Biol. Chem. 265 (32) (1990) 19758–19767.
[5] D.J. Thiel, M.H. le Du, R.L. Walter, A. D'Arcy, C. Chene, M. Fountoulakis, G. Garotta, F.K. Winkler, S.E. Ealick, Observation of an unexpected third receptor molecule in the crystal structure of human interferon-gamma receptor complex, Structure (London, England : 1993) 8 (9) (2000) 927–936.
[6] L.C. Platanias, Mechanisms of type-I- and type-II-interferon-mediated signalling, Nat. Rev. Immunol. 5 (5) (2005) 375–386.
[7] P. Mikulecký, J. Černý, L. Biedermannová, H. Petroková, M. Kuchař, J. Vondrášek, P. Malý, P. Šebo, B. Schneider, Increasing affinity of interferon-γ receptor 1 to interferon-γ by computer-aided design, BioMed Res. Int. 2013 (2013) 752514.
[8] J. Soh, R.J. Donnelly, T.M. Mariano, J.R. Cook, B. Schwartz, S. Pestka, Identification of a yeast artificial chromosome clone encoding an accessory factor for the human interferon gamma receptor: evidence for multiple accessory factors, Proc. Natl. Acad. Sci. U. S. A 90 (18) (1993) 8737–8741.
[9] P. Mikulecky, J. Zahradnik, P. Kolenko, J. Cerny, T. Charnavets, L. Kolarova, I. Necasova, P.N. Pham, B. Schneider, Crystal structure of human interferon-gamma receptor 2 reveals the structural basis for receptor specificity, Acta. Cryst. D, Struct. Biol. 72 (Pt 9) (2016) 1017–1025.
[10] X. Pang, H.-X. Zhou, A common model for cytokine receptor activation: combined scissor-like rotation and self-rotation of receptor dimer induced by class I cytokine, PLoS Comput. Biol. 8 (3) (2012) e1002427.
[11] R. Ferrao, Heidi J.A. Wallweber, H. Ho, C. Tam, Y. Franke, J. Quinn, Patrick J. Lupardus, The structural basis for class II cytokine receptor recognition by JAK1, Structure (London, England : 1993) 24 (6) (2016) 897–905.
[12] M. Sakatsume, K. Igarashi, K.D. Winestock, G. Garotta, A.C. Larner, D.S. Finbloom, The Jak kinases differentially associate with the alpha and beta (accessory factor) chains of the interferon gamma receptor to form a functional receptor unit capable of activating STAT transcription factors, J. Biol. Chem. 270 (29) (1995) 17528–17534.
[13] S.V. Kotenko, L.S. Izotova, B.P. Pollack, T.M. Mariano, R.J. Donnelly, G. Muthukumaran, J.R. Cook, G. Garotta, O. Silvennoinen, J.N. Ihle, et al., Interaction between the components of the interferon gamma receptor complex, J. Biol. Chem. 270 (36) (1995) 20915–20921.
[14] H.M. Johnson, E.N. Noon-Song, R. Dabelic, C.M. Ahmed, IFN signaling: how a non-canonical model led to the development of IFN mimetics, Front. Immunol. 4 (2013) 202.
[15] P.S. Subramaniam, M.M. Green, J. Larkin 3rd, B.A. Torres, H.M. Johnson, Nuclear translocation of IFN-gamma is an intrinsic requirement for its biologic activity and can be driven by a heterologous nuclear localization sequence, J. Interferon Cytokine Res. 21 (11) (2001) 951–959.
[16] W.P. Michalski, B.J. Shiell, T.E. O'Neil, G. Beddome, J.W. Lowenthal, Recombinant chicken IFN-gamma expressed in *Escherichia coli*: analysis of C-terminal truncation and effect on biologic activity, J. Interferon Cytokine Res. 19 (4) (1999) 383–392.
[17] T. Decker, P. Kovarik, A. Meinke, GAS elements: a few nucleotides with a major impact on cytokine-induced gene expression, J. Interferon Cytokine Res. 17 (3) (1997) 121–134.
[18] J.N. Volff, Genome evolution and biodiversity in teleost fish, Heredity 94 (3) (2004) 280–294.
[19] J.S. Taylor, I. Braasch, T. Frickey, A. Meyer, Y. Van de Peer, Genome duplication, a trait shared by 22,000 species of ray-finned fish, Genome Res. 13 (3) (2003) 382–390.
[20] A. Meyer, Y. Van de Peer, From 2R to 3R: evidence for a fish-specific genome duplication (FSGD), BioEssays 27 (9) (2005) 937–945.
[21] R. Savan, S. Ravichandran, J.R. Collins, M. Sakai, H.A. Young, Structural conservation of interferon gamma among vertebrates, Cytokine Growth Factor Rev. 20 (2) (2009) 115–124.
[22] C. Berthelot, F. Brunet, D. Chalopin, A. Juanchich, M. Bernard, B. Noel, P. Bento, C. Da Silva, K. Labadie, A. Alberti, J.M. Aury, A. Louis, P. Dehais, P. Bardou, J. Montfort, C. Klopp, C. Cabau, C. Gaspin, G.H. Thorgaard, M. Boussaha, E. Quillet, R. Guyomard, D. Galiana, J. Bobe, J.N. Volff, C. Genet, P. Wincker, O. Jaillon, H. Roest Crollius, Y. Guiguen, The rainbow trout genome provides novel insights into evolution after whole-genome duplication in vertebrates, Nat. Commun. 5 (2014) 3657.
[23] L. David, S. Blum, M.W. Feldman, U. Lavi, J. Hillel, Recent duplication of the common carp (*Cyprinus carpio* L.) genome as revealed by analyses of microsatellite loci, Mol. Biol. Evol. 20 (9) (2003) 1425–1434.
[24] M. Crane, A. Hyatt, Viruses of fish: an overview of significant pathogens, Viruses 3 (11) (2011) 2025–2046.
[25] B. Venkatesh, A.P. Lee, V. Ravi, A.K. Maurya, M.M. Lian, J.B. Swann, Y. Ohta, M.F. Flajnik, Y. Sutoh, M. Kasahara, S. Hoon, V. Gangu, S.W. Roy, M. Irimia, V. Korzh, I. Kondrychyn, Z.W. Lim, B.-H. Tay, S. Tohari, K.W. Kong, S. Ho, B. Lorente-Galdos, J. Quilez, T. Marques-Bonet, B.J. Raney, P.W. Ingham, A. Tay, L.W. Hillier, P. Minx, T. Boehm, R.K. Wilson, S. Brenner, W.C. Warren, Elephant shark genome provides unique insights into gnathostome evolution, Nature 505 (7482) (2014) 174–179.
[26] J. Zou, Y. Yoshiura, J.M. Dijkstra, M. Sakai, M. Ototake, C. Secombes, Identification of an interferon gamma homologue in Fugu, *Takifugu rubripes*, Fish Shellfish Immunol. 17 (4) (2004) 403–409.
[27] D. Igawa, M. Sakai, R. Savan, An unexpected discovery of two interferon gamma-like genes along with interleukin (IL)-22 and -26 from teleost: IL-22 and -26 genes have been described for the first time outside mammals, Mol. Immunol. 43 (7) (2006) 999–1009.
[28] B. Robertsen, V. Bergan, T. Rokenes, R. Larsen, A. Albuquerque, Atlantic salmon interferon genes: cloning, sequence analysis, expression, and biological activity, J. Interferon Cytokine Res. 23 (10) (2003) 601–612.
[29] E.H. Stolte, H.F. Savelkoul, G. Wiegertjes, G. Flik, B.M. Lidy, Verburg-van Kemenade, Differential expression of two interferon-gamma genes in common carp (*Cyprinus carpio* L.), Dev. Comp. Immunol. 32 (12) (2008) 1467–1481.
[30] M.K. Purcell, K.J. Laing, J.C. Woodson, G.H. Thorgaard, J.D. Hansen, Characterization of the interferon genes in homozygous rainbow trout reveals two novel genes, alternate splicing and differential regulation of duplicated genes, Fish Shellfish Immunol. 26 (2) (2009) 293–304.
[31] J. Zou, A. Carrington, B. Collet, J.M. Dijkstra, Y. Yoshiura, N. Bols, C. Secombes, Identification and bioactivities of IFN-gamma in rainbow trout *Oncorhynchus mykiss*: the first Th1-type cytokine characterized functionally in fish, J. Imunol. (Baltimore, Md.: 1950) 175 (4) (2005) 2484–2494.
[32] Y. Xiang, W. Liu, P. Jia, Y. Li, Y. Jin, L. Chen, J. Zhang, K. Jia, M. Yi, Molecular characterization and expression analysis of interferon-gamma in black seabream *Acanthopagrus schlegelii*, Fish Shellfish Immunol. 70 (2017) 140–148.
[33] S. Yoon, A. Alnabulsi, T.Y. Wang, P.T. Lee, T.Y. Chen, S. Bird, J. Zou, C.J. Secombes, Analysis of interferon gamma protein expression in zebrafish (*Danio rerio*), Fish Shellfish Immunol. 57 (2016) 79–86.
[34] S. Yang, Q. Li, Y. Mu, J. Ao, X. Chen, Functional activities of interferon gamma in large yellow croaker *Larimichthys crocea*, Fish Shellfish Immunol. 70 (2017) 545–552.
[35] C. Furnes, M. Seppola, B. Robertsen, Molecular characterisation and expression analysis of interferon gamma in Atlantic cod (*Gadus morhua*), Fish Shellfish Immunol. 26 (2) (2009) 285–292.
[36] J. Velazquez, J. Acosta, N. Herrera, A. Morales, O. Gonzalez, F. Herrera, M.P. Estrada, Y. Carpio, Novel IFNgamma homologue identified in Nile tilapia (*Oreochromis niloticus*) links with immune response in gills under different stimuli, Fish Shellfish Immunol. 71 (2017) 275–285.
[37] A.-C. Øvergård, I. Nepstad, A.H. Nerland, S. Patel, Characterisation and expression analysis of the Atlantic halibut (*Hippoglossus hippoglossus* L.) cytokines: IL-1β, IL-6, IL-11, IL-12β and IFNγ, Mol. Biol. Rep. 39 (3) (2012) 2201–2213.

[38] B.Y. Ruan, S.N. Chen, J. Hou, B. Huang, Z.A. Laghari, L. Li, P. Nie, Two type II IFN members, IFN-gamma and IFN-gamma related (rel), regulate differentially IRF1 and IRF11 in zebrafish, Fish Shellfish Immunol. 65 (2017) 103–110.
[39] W.Q. Chen, Q.Q. Xu, M.X. Chang, J. Zou, C.J. Secombes, K.M. Peng, P. Nie, Molecular characterization and expression analysis of the IFN-gamma related gene (IFN-gammarel) in grass carp *Ctenopharyngodon idella*, Vet. Immunol. Immunopathol. 134 (3–4) (2010) 199–207.
[40] L. Grayfer, M. Belosevic, Molecular characterization, expression and functional analysis of goldfish (*Carassius aurutus* L.) interferon gamma, Dev. Comp. Immunol. 33 (2) (2009) 235–246.
[41] I. Milev-Milovanovic, S. Long, M. Wilson, E. Bengten, N.W. Miller, V.G. Chinchar, Identification and expression analysis of interferon gamma genes in channel catfish, Immunogenetics 58 (1) (2006) 70–80.
[42] J.A. Arts, E.J. Tijhaar, M. Chadzinska, H.F. Savelkoul, B.M. Verburg-van Kemenade, Functional analysis of carp interferon-gamma: evolutionary conservation of classical phagocyte activation, Fish Shellfish Immunol. 29 (5) (2010) 793–802.
[43] J. Zou, C.J. Secombes, The function of fish cytokines, Biology 5 (2) (2016).
[44] D. Lu, T. Wang, X. Zhang, T. Leng, Y. Zhang, H. Lin, A comparative study of two interferon gamma in the regulation of tetraodon TLR recognition system, Fish Shellfish Immunol. 34 (6) (2013) 1662–1663.
[45] Y. Shibasaki, T. Yabu, K. Araki, N. Mano, H. Shiba, T. Moritomo, T. Nakanishi, Peculiar monomeric interferon gammas, IFNγrel 1 and IFNγrel 2, in ginbuna crucian carp, FEBS J. 281 (4) (2014) 1046–1056.
[46] D. Stuber, A. Friedlein, M. Fountoulakis, H.W. Lahm, G. Garotta, Alignment of disulfide bonds of the extracellular domain of the interferon gamma receptor and investigation of their role in biological activity, Biochemistry 32 (9) (1993) 2423–2430.
[47] J.C. Renauld, Class II cytokine receptors and their ligands: key antiviral and inflammatory modulators, Nat. Rev. Immunol. 3 (8) (2003) 667–676.
[48] A. Celada, R.D. Schreiber, Role of protein kinase C and intracellular calcium mobilization in the induction of macrophage tumoricidal activity by interferon-gamma, J. Immunol. 137 (7) (1986) 2373.
[49] D. Watling, D. Guschin, M. Muller, O. Silvennoinen, B.A. Witthuhn, F.W. Quelle, N.C. Rogers, C. Schindler, G.R. Stark, J.N. Ihle, I.M. Kerr, Complementation by the protein tyrosine kinase JAK2 of a mutant cell line defective in the interferon-γ signal transduction pathway, Nature 366 (6451) (1993) 166–170.
[50] C.V. Ramana, M.P. Gil, R.D. Schreiber, G.R. Stark, Stat1-dependent and -independent pathways in IFN-γ-dependent signaling, Trends Immunol. 23 (2) (2002) 96–101.
[51] K. Igarashi, G. Garotta, L. Ozmen, A. Ziemiecki, A.F. Wilks, A.G. Harpur, A.C. Larner, D.S. Finbloom, Interferon-gamma induces tyrosine phosphorylation of interferon-gamma receptor and regulated association of protein tyrosine kinases, Jak1 and Jak2, with its receptor, J. Biol. Chem. 269 (20) (1994) 14333–14336.
[52] S.D. Rosenzweig, O.M. Schwartz, M.R. Brown, T.L. Leto, S.M. Holland, Characterization of a dipeptide motif regulating IFN-gamma receptor 2 plasma membrane accumulation and IFN-gamma responsiveness, J. Immunol. (Baltimore, Md.: 1950) 173 (6) (2004) 3991–3999.
[53] D. Aggad, C. Stein, D. Sieger, M. Mazel, P. Boudinot, P. Herbomel, J.-P. Levraud, G. Lutfalla, M. Leptin, Vivo analysis of Ifn-γ1 and Ifn-γ2 signaling in zebrafish, J. Immunol. 185 (11) (2010) 6774–6782.
[54] Q. Gao, P. Nie, K.D. Thompson, A. Adams, T. Wang, C.J. Secombes, J. Zou, The search for the IFN-gamma receptor in fish: functional and expression analysis of putative binding and signalling chains in rainbow trout *Oncorhynchus mykiss*, Dev. Comp. Immunol. 33 (8) (2009) 920–931.
[55] L. Grayfer, M. Belosevic, M. Belosevic, Molecular characterization of novel interferon gamma receptor 1 isoforms in zebrafish (*Danio rerio*) and goldfish (*Carassius auratus* L.), Mol. Immunol. 46 (15) (2009) 3050–3059.
[56] T. Unger, Y. Jacobovitch, A. Dantes, R. Bernheim, Y. Peleg, Applications of the Restriction Free (RF) cloning procedure for molecular manipulations and protein expression, J. Struct. Biol. 172 (1) (2010) 34–44.
[57] A. Erijman, A. Dantes, R. Bernheim, J.M. Shifman, Y. Peleg, Transfer-PCR (TPCR): a highway for DNA cloning and protein engineering, J. Struct. Biol. 175 (2) (2011) 171–177.
[58] Z. Luo, Selenourea: a convenient phasing vehicle for macromolecular X-ray crystal structures, Sci. Rep. 6 (2016) 37123.
[59] H.M. Berman, T. Battistuz, T.N. Bhat, W.F. Bluhm, P.E. Bourne, K. Burkhardt, Z. Feng, G.L. Gilliland, L. Iype, S. Jain, P. Fagan, J. Marvin, D. Padilla, V. Ravichandran, B. Schneider, N. Thanki, H. Weissig, J.D. Westbrook, C. Zardecki, The protein data bank, Acta. Cryst. D 58 (Pt 6 No 1) (2002) 899–907.
[60] S.E. Ealick, W.J. Cook, S. Vijay-Kumar, M. Carson, T.L. Nagabhushan, P.P. Trotta, C.E. Bugg, Three-dimensional structure of recombinant human interferon-gamma, Science 252 (5006) (1991) 698–702.
[61] A.A. Nuara, L.J. Walter, N.J. Logsdon, S.I. Yoon, B.C. Jones, J.M. Schriewer, R.M. Buller, M.R. Walter, Structure and mechanism of IFN-gamma antagonism by an orthopoxvirus IFN-gamma-binding protein, Proc. Natl. Acad. Sci. U. S. A 105 (6) (2008) 1861–1866.
[62] C.T. Samudzi, L.E. Burton, J.R. Rubin, Crystal structure of recombinant rabbit interferon-gamma at 2.7-A resolution, J. Biol. Chem. 266 (32) (1991) 21791–21797.
[63] M. Randal, A.A. Kossiakoff, The 2.0 A structure of bovine interferon-gamma; assessment of the structural differences between species, Acta. Cryst. D 56 (Pt 1) (2000) 14–24.
[64] C.T. Samudzi, J.R. Rubin, Structure of recombinant bovine interferon-gamma at 3.0 A resolution, Acta. Cryst. D 49 (Pt 6) (1993) 513–521.
[65] W. Kabsch, XDS, Acta. Crystallogr. D Biol. Crystallogr. 66 (Pt 2) (2010) 125–132.
[66] P.R. Evans, G.N. Murshudov, How good are my data and what is the resolution? Acta. Cryst. D 69 (Pt 7) (2013) 1204–1214.
[67] M.D. Winn, C.C. Ballard, K.D. Cowtan, E.J. Dodson, P. Emsley, P.R. Evans, R.M. Keegan, E.B. Krissinel, A.G. Leslie, A. McCoy, S.J. McNicholas, G.N. Murshudov, N.S. Pannu, E.A. Potterton, H.R. Powell, R.J. Read, A. Vagin, K.S. Wilson, Overview of the CCP4 suite and current developments, Acta. Cryst. D 67 (Pt 4) (2011) 235–242.
[68] G.M. Sheldrick, Experimental phasing with SHELXC/D/E: combining chain tracing with density modification, Acta. Crystallogr. D Biol. Crystallogr. 66 (Pt 4) (2010) 479–485.
[69] G.G. Langer, S. Hazledine, T. Wiegels, C. Carolan, V.S. Lamzin, Visual automated macromolecular model building, Acta. Cryst. D 69 (Pt 4) (2013) 635–641.
[70] P. Emsley, B. Lohkamp, W.G. Scott, K. Cowtan, Features and development of coot, Acta. Cryst. D 66 (Pt 4) (2010) 486–501.
[71] G.N. Murshudov, P. Skubak, A.A. Lebedev, N.S. Pannu, R.A. Steiner, R.A. Nicholls, M.D. Winn, F. Long, A.A. Vagin, REFMAC5 for the refinement of macromolecular crystal structures, Acta. Cryst. D 67 (Pt 4) (2011) 355–367.
[72] V.B. Chen, W.B. Arendall 3rd, J.J. Headd, D.A. Keedy, R.M. Immormino, G.J. Kapral, L.W. Murray, J.S. Richardson, D.C. Richardson, MolProbity: all-atom structure validation for macromolecular crystallography, Acta. Cryst. D 66 (Pt 1) (2010) 12–21.
[73] D.G. Gibson, L. Young, R.-Y. Chuang, J.C. Venter, C.A. Hutchison, H.O. Smith, Enzymatic assembly of DNA molecules up to several hundred kilobases, Nat. Meth. 6 (5) (2009) 343–345.
[74] O. Plihal, J. Sklenar, J. Kmonickova, P. Man, P. Pompach, V. Havlicek, V. Kren, K. Bezouska, N-glycosylated catalytic unit meets O-glycosylated propeptide: complex protein architecture in a fungal hexosaminidase, Biochem. Soc. Trans. 32 (Pt 5) (2004) 764–765.
[75] P. Pompach, P. Man, D. Kavan, K. Hofbauerová, V. Kumar, K. Bezouška, V. Havlíček, P. Novák, Modified electrophoretic and digestion conditions allow a simplified mass spectrometric evaluation of disulfide bonds, J. Mass Spect. 44 (11) (2009) 1571–1578.
[76] G. Bohm, R. Muhr, R. Jaenicke, Quantitative analysis of protein far UV circular dichroism spectra by neural networks, Prot. Eng. 5 (3) (1992) 191–195.
[77] D. Franke, A.G. Kikhney, D.I. Svergun, Automated acquisition and analysis of small angle X-ray scattering data, Nucl. Instrum. Met. Phys. Res. A 689 (2012) 52–59.
[78] P.V. Konarev, V.V. Volkov, A.V. Sokolova, M.H.J. Koch, D.I. Svergun, PRIMUS: a Windows PC-based system for small-angle scattering data analysis, J. Appl. Crystallogr. 36 (2003) 1277–1282.
[79] D. Svergun, Determination of the regularization parameter in indirect-transform methods using perceptual criteria, J. Appl. Crystallogr. 25 (4) (1992) 495–503.
[80] S.F. Altschul, W. Gish, W. Miller, E.W. Myers, D.J. Lipman, Basic local alignment search tool, J. Mol. Biol. 215 (3) (1990) 403–410.
[81] G.S.C. Slater, E. Birney, Automated generation of heuristics for biological sequence comparison, BMC Bioinf. 6 (1) (2005) 31.
[82] R.C. Edgar, MUSCLE: multiple sequence alignment with high accuracy and high throughput, Nucleic Acids Res. 32 (5) (2004) 1792–1797.
[83] A. Krogh, B. Larsson, G. von Heijne, E.L. Sonnhammer, Predicting transmembrane protein topology with a hidden Markov model: application to complete genomes, J. Mol. Biol. 305 (3) (2001) 567–580.
[84] O. Emanuelsson, S. Brunak, G. von Heijne, H. Nielsen, Locating proteins in the cell using TargetP, signalP and related tools, Nat. Protocols 2 (4) (2007) 953–971.
[85] S. Capella-Gutierrez, J.M. Silla-Martinez, T. Gabaldon, trimAl: a tool for automated alignment trimming in large-scale phylogenetic analyses, Bioinformatics (Oxford, England) 25 (15) (2009) 1972–1973.
[86] J.P. Huelsenbeck, F. Ronquist, MRBAYES: Bayesian inference of phylogenetic trees, Bioinformatics (Oxford, England) 17 (8) (2001) 754–755.
[87] F. Abascal, R. Zardoya, D. Posada, ProtTest: selection of best-fit models of protein evolution, Bioinformatics (Oxford, England) 21 (9) (2005) 2104–2105.
[88] S. Guindon, J.F. Dufayard, V. Lefort, M. Anisimova, W. Hordijk, O. Gascuel, New algorithms and methods to estimate maximum-likelihood phylogenies: assessing the performance of PhyML 3.0, Syst. Biol. 59 (3) (2010) 307–321.
[89] V. Lefort, J.E. Longueville, O. Gascuel, SMS: smart model selection in PhyML, Mol. Biol. Evol. 34 (9) (2017) 2422–2424.
[90] B.C. Stover, K.F. Muller, TreeGraph 2: combining and visualizing evidence from different phylogenetic analyses, BMC Bioinf. 11 (2010) 7.
[91] T.M. Nye, P. Lio, W.R. Gilks, A novel algorithm and web-based tool for comparing two alternative phylogenetic trees, Bioinformatics (Oxford, England) 22 (1) (2006) 117–119.
[92] P. Legendre, Y. Desdevises, E. Bazin, R.D.M. Page, A statistical test for host–parasite coevolution, Syst. Biol. 51 (2) (2002) 217–234.
[93] E. Paradis, J. Claude, K. Strimmer, APE: analyses of phylogenetics and evolution in R language, Bioinformatics (Oxford, England) 20 (2) (2004) 289–290.
[94] L.J. Revell, Phytools: an R package for phylogenetic comparative biology (and other things), Methods Ecol. Evol. 3 (2) (2012) 217–223.
[95] J. Iserte, F.L. Simonetti, D.J. Zea, E. Teppa, C. Marino-Buslje, I-COMS: interprotein-correlated mutations server, Nucleic Acids Res. 43 (W1) (2015) W320–W325.
[96] E.F. Pettersen, T.D. Goddard, C.C. Huang, G.S. Couch, D.M. Greenblatt, E.C. Meng, T.E. Ferrin, UCSF chimera–a visualization system for exploratory research and analysis, J. Comput. Chem. 25 (13) (2004) 1605–1612.
[97] W.R. Pearson, An Introduction to Sequence Similarity ("Homology") Searching, Current Protocols in Bioinformatics, John Wiley & Sons, Inc., 2002.
[98] W.R. Pearson, Selecting the Right Similarity-scoring Matrix, Current Protocols in Bioinformatics, John Wiley & Sons, Inc., 2002.

[99] M.A. Marti-Renom, A.C. Stuart, A. Fiser, R. Sanchez, F. Melo, A. Sali, Comparative protein structure modeling of genes and genomes, Annu. Rev. Biophys. 29 (2000) 291–325.
[100] A. Fiser, R.K. Do, A. Sali, Modeling of loops in protein structures, Protein Sci.: a Publ. Prot. Soc. 9 (9) (2000) 1753–1773.
[101] Z. Ping, J. Qi, Y. Sun, G. Lu, Y. Shi, X. Wang, G.F. Gao, M. Wang, Crystal structure of the interferon gamma receptor alpha chain from chicken reveals an undetected extra helix compared with the human counterparts, J. Interferon Cytokine Res. 34 (1) (2014) 41–51.
[102] A. Sali, T.L. Blundell, Comparative protein modelling by satisfaction of spatial restraints, J. Mol. Biol. 234 (3) (1993) 779–815.
[103] T. Matsuyama, A. Fujiwara, T. Sakai, C. Nakayasu, Molecular cloning and expression analysis of interferon gamma gene in Japanese flounder *Paralichthys olivaceus*, Fish Sci. 75 (1) (2009) 253–255.
[104] T.J. Near, R.I. Eytan, A. Dornburg, K.L. Kuhn, J.A. Moore, M.P. Davis, P.C. Wainwright, M. Friedman, W.L. Smith, Resolution of ray-finned fish phylogeny and timing of diversification, Proc. Natl. Acad. Sci. U.S.A. 109 (34) (2012) 13698–13703.
[105] T.H. Ogden, M.S. Rosenberg, Multiple sequence alignment accuracy and phylogenetic inference, Syst. Biol. 55 (2) (2006) 314–328.
[106] B.G. Hall, Comparison of the accuracies of several phylogenetic methods using protein and DNA sequences, Mol. Biol. Evol. 22 (3) (2005) 792–802.
[107] Y.H. Loh, L.S. Katz, M.C. Mims, T.D. Kocher, S.V. Yi, J.T. Streelman, Comparative analysis reveals signatures of differentiation amid genomic polymorphism in Lake Malawi cichlids, Genome Biol. 9 (7) (2008) R113.
[108] P. Xu, X. Zhang, X. Wang, J. Li, G. Liu, Y. Kuang, J. Xu, X. Zheng, L. Ren, G. Wang, Y. Zhang, L. Huo, Z. Zhao, D. Cao, C. Lu, C. Li, Y. Zhou, Z. Liu, Z. Fan, G. Shan, X. Li, S. Wu, L. Song, G. Hou, Y. Jiang, Z. Jeney, D. Yu, L. Wang, C. Shao, L. Song, J. Sun, P. Ji, J. Wang, Q. Li, L. Xu, F. Sun, J. Feng, C. Wang, S. Wang, B. Wang, Y. Li, Y. Zhu, W. Xue, L. Zhao, J. Wang, Y. Gu, W. Lv, K. Wu, J. Xiao, J. Wu, Z. Zhang, J. Yu, X. Sun, Genome sequence and genetic diversity of the common carp, *Cyprinus carpio*, Nat. Genet. 46 (11) (2014) 1212–1219.
[109] S.-I. Yoon, B.C. Jones, N.J. Logsdon, B.D. Harris, A. Deshpande, S. Radaeva, B.A. Halloran, B. Gao, M.R. Walter, Structure and mechanism of receptor sharing by the IL-10R2 common chain, Structure (London, England: 1993) 18 (5) (2010) 638–648.
[110] N.J. Logsdon, A. Deshpande, B.D. Harris, K.R. Rajashankar, M.R. Walter, Structural basis for receptor sharing and activation by interleukin-20 receptor-2 (IL-20R2) binding cytokines, Proc. Natl. Acad. Sci. U. S. A 109 (31) (2012) 12704–12709.
[111] D. Talavera, S.C. Lovell, S. Whelan, Covariation is a poor measure of molecular coevolution, Mol. Biol. Evol. 32 (9) (2015) 2456–2468.
[112] R. Sabat, IL-10 family of cytokines, Cytokine Growth Factor Rev. 21 (5) (2010) 315–324.
[113] J.A. Langer, E.C. Cutrone, S. Kotenko, The class II cytokine receptor (CRF2) family: overview and patterns of receptor–ligand interactions, Cytokine Growth Factor Rev. 15 (1) (2004) 33–48.
[114] S. Pletnev, E. Magracheva, A. Wlodawer, A. Zdanov, A model of the ternary complex of interleukin-10 with its soluble receptors, BMC Struct. Biol. 5 (1) (2005) 10.